Journal of the Optical Society of Korea
Vol. 18, No. 4, August 2014, pp. 341-344

ISSN: 1226-4776(Print) / ISSN: 2093-6885(Online)
DOI: http://dx.doi.org/10.3807/JOSK.2014.18.4.341

Modified Sub-aperture Stitching Algorithm using Image Sharpening and Particle Swarm Optimization

Yiwei Chen[1,2]*, Erlong Miao[1], Yongxin Sui[1], and Huaijiang Yang[1]

[1]*State Key Laboratory of Applied Optics, Changchun Institute of Optics, Fine Mechanics and Physics, Chinese Academy of Sciences, Changchun, Jilin 130033, China*
[2]*University of Chinese Academy of Sciences, Beijing 100049, China*

(Received March 17, 2014 : revised May 7, 2014 : accepted June 9, 2014)

This study proposes a modified sub-aperture stitching algorithm, which uses an image sharpening algorithm and particle swarm optimization to improve the stitching accuracy. In sub-aperture stitching interferometers with high positional accuracy, the high-frequency components of measurements are more important than the low-frequency components when compensating for position errors using a sub-aperture stitching algorithm. Thus we use image sharpening algorithms to strengthen the high-frequency components of measurements. When using image sharpening algorithms, sub-aperture stitching algorithms based on the least-squares method easily become trapped at locally optimal solutions. However, particle swarm optimization is less likely to become trapped at a locally optimal solution, thus we utilized this method to develop a more robust algorithm. The results of simulations showed that our algorithm compensated for position errors more effectively than the existing algorithm. An experimental comparison with full aperture-testing results demonstrated the validity of the new algorithm.

Keywords : Image sharpening, Optical testing, Particle swarm optimization, Sub-aperture stitching
OCIS codes : (220.4840) Testing; (120.3180) Interferometry; (120.6650) Surface measurements, figure; (120.4630) Optical inspection

I. INTRODUCTION

In the development of astronomical optics, space optics [1-3], and inertial confinement fusion, large-aperture optical systems have been widely used. With long production cycle and high cost, large-aperture interferometers cannot satisfy the advanced requirements for testing large optical elements. In 1982, Kim addressed this problem by developing the sub-aperture stitching method [4]. The core of this method is stitching together the measurements obtained from all of the sub-apertures to generate the full-aperture result. However, location errors are inevitable when using this method, so researchers use the overlapping areas between sub-apertures to compensate for the location errors [5-8]. The location errors include piston, tilt, defocus, clocking, and position errors. Piston, tilt, and defocus errors are easily compensated, and clocking errors are usually quite small, but position errors are not usually compensated well by algorithms. In most cases sub-aperture stitching interferometers have high positional accuracy, so the high-frequency components of measurements are the key factors when compensating for position errors. Therefore, we use an image sharpening algorithm to strengthen the high-frequency components of measurements. The basis of image sharpening is computing the approximate gradient of a measurement, so that the data may be stripped of many low-frequency components after image sharpening. However, the low-frequency components are helpful in avoiding local minima, and a sub-aperture stitching algorithm based on the least-squares method can easily become trapped at a local minimum if the image is sharpened. A different optimization algorithm should be used to solve this problem.

Some researchers have used particle swarm optimization to address this problem in image stitching [9]. Particle swarm optimization can be more reliable than the least-squares method for finding the globally optimal solution. Therefore, we utilize particle swarm optimization in our

*Corresponding author: cyw198788@163.com
Color versions of one or more of the figures in this paper are available online.

algorithm to calculate the position compensation. In Section II we introduce an existing iterative sub-aperture stitching algorithm based on the least-squares method, while in Section III we describe our modified sub-aperture stitching algorithm, which uses image sharpening and particle swarm optimization. In Section IV we present the results of simulations comparing the performance of the two algorithms, and in Section V we report experimental results that demonstrate the effectiveness of the proposed method. Section VI presents our conclusions.

II. ITERATIVE SUB-APERTURE STITCHING ALGORITHM BASED ON THE LEAST-SQUARES METHOD

For convenience, in this article we discuss the testing of only plano-optical elements. First, a sub-aperture (usually the central one) is selected as the reference sub-aperture. Clearly the other sub-apertures have tilt and piston relative to the reference sub-aperture, as shown in Fig. 1. Thus it is necessary to compensate for the relative tilt and piston [5-7]:

$$z_i^*(x,y) = z_i(x,y) + a_i x + b_i y + c_i \tag{1}$$

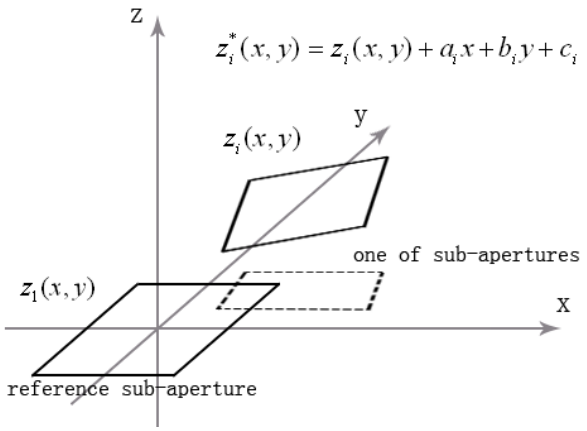

FIG. 1. Measurement of the *i*th sub-aperture in terms of the tilt and piston.

where $z_i(x,y)$ is the measured value of the *i*th sub-aperture, $z_i^*(x,y)$ is the value after compensation, a_i and b_i are the coefficients of the relative tilt for the *i*th sub-aperture in the x and y directions respectively, and c_i is the coefficient of the relevant piston for the *i*th sub-aperture .

The sub-aperture stitching interferometer possesses six types of mechanical location errors, and the other errors must also be compensated. For the x-position error (shown in Fig. 2(a)), y-position error (shown in Fig. 2(b)), and clocking error (shown in Fig. 2(c)) of the *i*th sub-aperture, the value after compensation is (using linear approximation) [8]:

$$z_i^*(x,y) = z_i(x,y) + a_i x + b_i y + c_i + \frac{\partial z_i(x,y)}{\partial x}\Delta x_i + \frac{\partial z_i(x,y)}{\partial y}\Delta y_i + \frac{\partial z_i(x,y)}{\partial \theta}\Delta\theta_i \tag{2}$$

where θ is the angle of the *i*th sub-aperture.

Assuming that there are N sub-apertures, where the reference sub-aperture is number 1, the sub-apertures (except number 1) have to be compensated in terms of their tilt, piston, x-position error, y-position error, and clocking error to minimize the difference in the sub-aperture overlapping area between adjacent sub-apertures. The least-squares method is used [8], as follows.

$$\begin{aligned}\min = \sum_{i=2}^{i\neq 1}\sum_{j=i\ldots N}^{j\neq 1} &((z_i(x,y) + a_i x + b_i y + c_i + \frac{\partial z_i(x,y)}{\partial x}\Delta x_i + \frac{\partial z_i(x,y)}{\partial y}\Delta y_i + \frac{\partial z_i(x,y)}{\partial \theta}\Delta\theta_i) \\ &-(z_j(x,y) + a_j x + b_j y + c_j + \frac{\partial z_j(x,y)}{\partial x}\Delta x_j + \frac{\partial z_j(x,y)}{\partial y}\Delta y_j + \frac{\partial z_j(x,y)}{\partial \theta}\Delta\theta_j))^2 \\ &+ \sum_{k=2\ldots N}^{k\neq 1} ((z_k(x,y) + a_k x + b_k y + c_k + \frac{\partial z_k(x,y)}{\partial x}\Delta x_k + \frac{\partial z_k(x,y)}{\partial y}\Delta y_k + \frac{\partial z_k(x,y)}{\partial \theta}\Delta\theta_k) - z_1(x,y))^2\end{aligned} \tag{3}$$

Since linear approximation is used to solve the nonlinear problem described above, an iterative algorithm can be used [8]: alternately use overlapping sub-aperture areas to calculate compensation values, and use compensation values to calculate overlapping aperture areas.

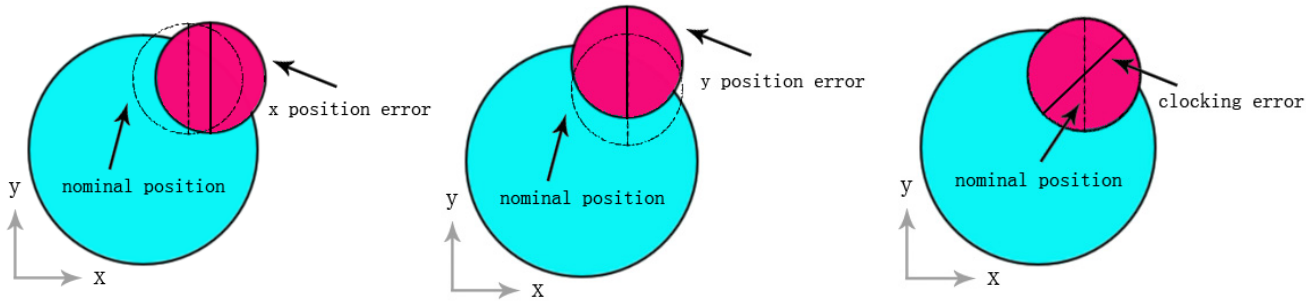

(a) (b) (c)

FIG. 2. Mechanical location errors of the *i*th sub-aperture: (a) x-position error, (b) y-position error, (c) clocking error.

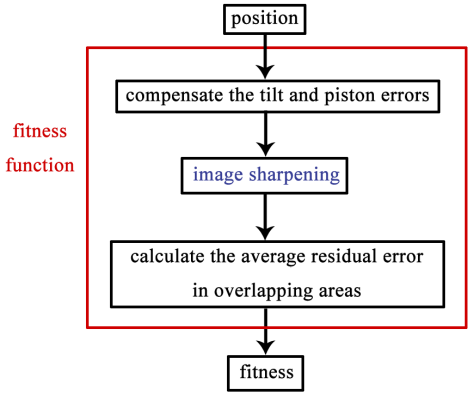

FIG. 3. Flowchart showing the process used to calculate the fitness of each particle.

III. MODIFIED SUB-APERTURE STITCHING ALGORITHM USING IMAGE SHARPENING AND PARTICLE SWARM OPTIMIZATION

Before discussing our algorithm, we provide brief descriptions of image sharpening and particle swarm optimization.

Image sharpening is a technique that reinforces the high-frequency components of images, and there are many different image sharpening algorithms [10, 11]. We use an image sharpening algorithm based on the Sobel operator [12], a famous gradient operator which is widely used in image processing.

Reference 13 states the following: "Particle swarm optimization is a computational intelligence-based technique that is not largely affected by the size and nonlinearity of the problem, and can converge to the optimal solution in many problems where most analytical methods fail to converge."

In our algorithm we select the position value indicated by the instrument as the initial candidate solution, and the range of allowable errors is used as the search space for particle swarm optimization.

A flowchart of the process used to calculate the fitness of each particle is shown in Fig. 3. The least-squares method is used to compensate for the tilt and piston errors [5, 6], and the fitness is the average residual error in the overlapping areas. After clarifying the variables and fitness function, we use the particle swarm optimization algorithm to calculate the positions of the sub-apertures. After the positions of the sub-apertures have been determined, the stitching result can be calculated using the algorithm described by Otsubo et al. [6].

IV. SIMULATION

In the simulation, a measurement (301 × 301 pixels, as shown in Fig. 4) was divided into seven sub-apertures (Fig. 5), which were then stitched together using both the existing algorithm and our proposed algorithm.

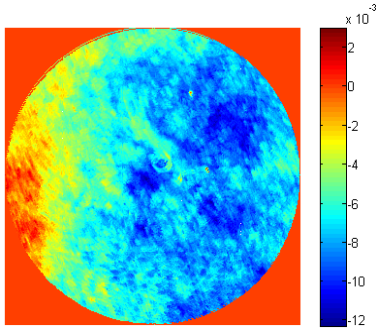

FIG. 4. Measurement results. (unit: wavelength)

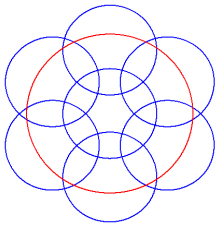

FIG. 5. Layout of the sub-apertures (blue) used to analyze a large aperture objective (red).

TABLE 1. Simulation results. All units are the length of one pixel

Width	0.2	0.4	0.6	0.8	1
Initial Error	0.06295	0.1259	0.1888	0.2084	0.2518
Existing Algorithm	0.5625	0.4887	0.8130	0.2726	0.3570
Proposed Algorithm	0.03784	0.03785	0.05940	0.06700	0.09004

After dividing the measured image into sub-apertures, we added random noise ([-0.0002, 0.0002] wavelength) and the piston, tilt, and position errors to each sub-aperture. The position errors were random lengths between -Width/2 and Width/2, where Width was a parameter used in the simulation.

To evaluate the performance of the two algorithms with increasing values of position errors, the simulation results are compared in Table 1, where the initial error is the variance in the initial position errors. In the table the results for the existing and proposed algorithms show the variance in the position errors based on simulations using the respective algorithms. The existing algorithm could not compensate for position errors when Width was less than one pixel, whereas the proposed method performed quite well.

V. EXPERIMENT

Using the layout of sub-apertures shown in Fig. 6, a flat surface (caliber = 150 mm) was measured with a

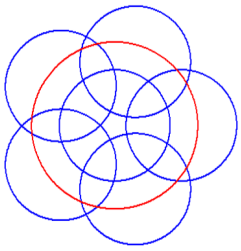

FIG. 6. Layout of the sub-apertures.

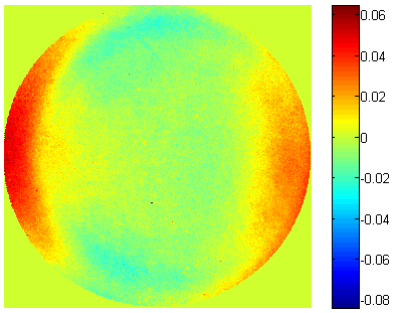

(a)

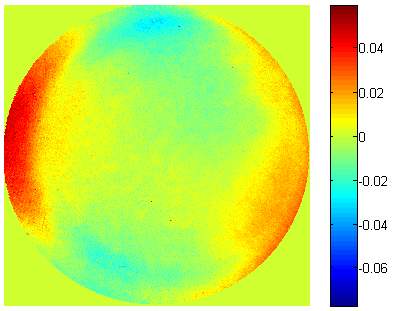

(b)

FIG. 7. Experimental results: (a) stitched using our algorithm, (b) full-aperture measurement. (unit: wavelength)

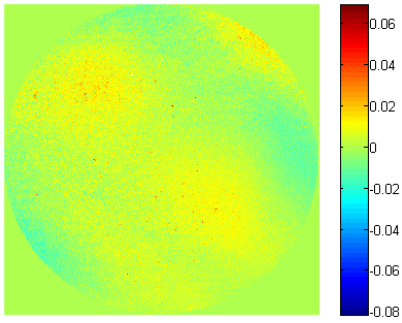

FIG. 8. Residual error. (unit: wavelength)

sub-aperture stitching interferometer (caliber = 100 mm). The measurement results obtained with a full-aperture using our algorithm are shown in Fig. 7(a). For the measurement results obtained using an interferometer with a caliber of 150 mm (shown in Fig. 7(b)), the root mean squared error was 0.006372 λ and the residual error image is shown in Fig. 8.

VI. CONCLUSION

In this study we proposed a modified sub-aperture stitching algorithm, which uses image sharpening algorithms and particle swarm optimization to improve the stitching accuracy for sub-aperture stitching interferometers with high positional accuracy. The results of simulations demonstrated that the proposed algorithm performs better than the existing method. A comparison with experimental full-aperture testing results demonstrated the validity of the proposed algorithm.

REFERENCES

1. X. L. Li, M. Xu, X. D. Ren, and Y. T. Pei, "An optical design of off-axis four-mirror-anastigmatic telescope for remote sensing," J. Opt. Soc. Korea **16**, 243-246 (2012).
2. X. L. Li, M. Xu, and Y. T. Pei, "Optical design of an off-axis five-mirror-anastigmatic telescope for near infared remote sensing," J. Opt. Soc. Korea **16**, 343-348 (2012).
3. H. Jin, J. Lim, Y. Kim, and S. Kim, "Optical design of a reflecting telescope for cubesat," J. Opt. Soc. Korea **17**, 533-537 (2013).
4. C. J. Kim, "Polynomial fit of interferograms," Appl. Opt. **21**, 4521-4525 (1982).
5. M. Otsubo, K. Okada, and J. Tsujiuchi, "Measurement of large plane surface shape with interferometric aperture synthesis," Proc. SPIE **1720**, 444-447 (1992).
6. M. Otsubo, K. Okada, and J. Tsujiuchi, "Measurement of large plane surface shapes by connecting small-aperture," Opt. Eng. **33**, 608-613 (1994).
7. M. Sjödahl and B. F. Oreb, "Stitching interferometric measurement data for inspection of large optical components," Opt. Eng. **41**, 403-408 (2002).
8. D. Golini, G. Forbes, and P. Murphy, "Method for self-calibrated subaperture stitching for surface figure measurement," US Patent:6956657B (2005).
9. Y. Zhang and H. Zhou, "Image stitching based on particle swarm and maximum mutual information algorithm," Journal of Multimedia **8**, 580-587 (2013).
10. Z. Gui and Y. Liu, "An image sharpening algorithm based on fuzzy logic," Optik-International Journal for Light and Electron Optics **122**, 697-702 (2011).
11. J. Zeng, "An image sharpening algorithm based on edge detection," Modern Electronics Technique **12**, 033 (2006).
12. Y. D. Qu, C. S. Cui, S. B. Chen, and J.-Q. Li, "A fast subpixel edge detection method using Sobel-Zernike moments operator," Image and Vision Computing **23**, 11-17 (2005).
13. Y. del Valle, G. K. Venayagamoorthy, S. Mohagheghi, J.-C. Hernandez, and R. G. Harley, "Particle swarm optimization: Basic concepts, variants and application in power systems," IEEE Transactions on Evolutionary Computation **12**, 2 (2008).